Fabrication of transparent polysiloxane coatings on a glass support via the sol-gel dip coating technique and the effect of their hydrophobization with hexamethyldisilazane

Michał Chodkowski [1], Konrad Terpiłowski [1], Sylwia Pasieczna-Patkowska [2]

[1] Department of Interfacial Phenomena, Institute of Chemical Sciences, Faculty of Chemistry, Maria Curie-Skłodowska University in Lublin, pl. M. Curie-Skłodowskiej 3, 20-031 Lublin, Poland

[2] Department of Chemical Technology, Institute of Chemical Sciences, Faculty of Chemistry, Maria Curie-Skłodowska University in Lublin, pl. M. Curie-Skłodowskiej 3, 20-031 Lublin, Poland

Corresponding author: michal.chodkowski@poczta.umcs.lublin.pl (M. Chodkowski)

Abstract: This study aimed at synthesis, preparation, and physicochemical properties investigation of undoped polysiloxane-based coatings deposited on the glass supports. The other goal was to test the effectiveness of their hydrophobization with hexamethyldisilazane at an elevated temperature using a bubbler. The coatings were obtained in a sol-gel process by acid-assisted hydrolysis of tetraethoxysilane and they were applied to the glass supports using the dip coating technique with various withdrawal speeds. The synthesized composition was scanned using Turbiscan[LAB] and its particle size was determined by means of the dynamic light scattering technique. The obtained surfaces were examined based on the water wettability measurements, photoacoustic spectroscopy, and transmittance measurements. It was found that the stability of the sol did not change during the dip-coating. Smooth, homogeneous, uniform, hydrophobic, and transparent coatings on the glass supports were obtained. Their wettability was determined by the contact angle in the range from 83.5 to 95.2 degrees and very low contact angle hysteresis. The hydrophobic effect obtained by modification with hexamethyldisilazane appears to be permanent - the contact angles do not change significantly after 7 days. The synthesized sol composition appears to be a good starting point for its chemical and physical modification for hydrophobicity increase and surface properties modification. Moreover, the hydrophobization of the coatings with hexamethyldisilazane at an elevated temperature using the bubbler did not have the desired effect.

Keywords: silica, coating, hydrophobization, wettability, HMDS, bubbler

1. Introduction

Any modifications of a surface are most often aimed at improving its properties and functionality. There are different ways to do this, but coating application is the most common. The dip-coating technique seems to be the most suitable method for this purpose. Its advantages include, among others, low costs and ability to control the layer properties by its thickness. In combination with the sol-gel method, it is widely used for thin films deposition on the glass substrates. These types of coatings are usually based on the silica nanoparticles synthesized by the base-assisted organosilane precursor hydrolysis. However, they can also be obtained by the acid-assisted hydrolysis which leads to a polymeric form of the polysiloxane. Depending on the reaction conditions, the use of precursor and the modifiers, coatings with a wide range of properties can be obtained.

    The term polysiloxane refers to a polymer with a silicon-oxygen backbone while the term silica is used to describe the whole range of silicon-based materials. Polysiloxane coatings, also reported in the literature with the name of silica coatings, have several desirable properties. They can be highly

transparent and scratch resistant (Li et al., 2020), oleophobic (Yang et al., 2020), biocompatible (Legge et al., 2019), eco-friendly (Ibrahim and Sultan, 2020), hydrophilic or hydrophobic.

The hydrophobicity of a surface is the result of its chemical and physical properties. A chemical factor that promotes hydrophobicity is the presence of nonpolar surface functional groups such as alkyl groups or their fluorinated derivatives. They are not able to create a hydrogen bond with water molecules and make the surface free energy relatively low. The hydrophobicity of a surface is also influenced by its topography, namely by its roughness. There are two main methods for coating hydrophobization. The first one involves adding an appropriate modifier in the coating synthesis stage. In case of the silica ones it could be, for example, a polymer such as poly(dimethylsiloxane) which contains hydrophobic groups (Protsak et al., 2018). The roughening additive can be glass micro/nanoparticles or silica nanoparticles themselves. The second method of hydrophobization is the functionalisation of the coating after its application. It includes such methods as plasma treatment, chemical modification, or particle deposition. In the case of polysiloxane coatings and silica materials in general, surface hydrophobization with hexamethyldisilazane (HMDS) is often used. It employs a gas-phase process known as Chemical Vapor Deposition (CVD). The most common procedure involves keeping the surface in a desiccator under the HMDS saturated vapours, most often at room temperature (Yue et al., 2019) but there are also reports about the substrate immersion in the liquid HMDS (San Vincente et al., 2010). This reaction minimizes the number of hydrophilic silanol groups (−Si−OH) present on the surface by replacing them with the hydrophobic trimethylsilyl (TMS) groups as follows:
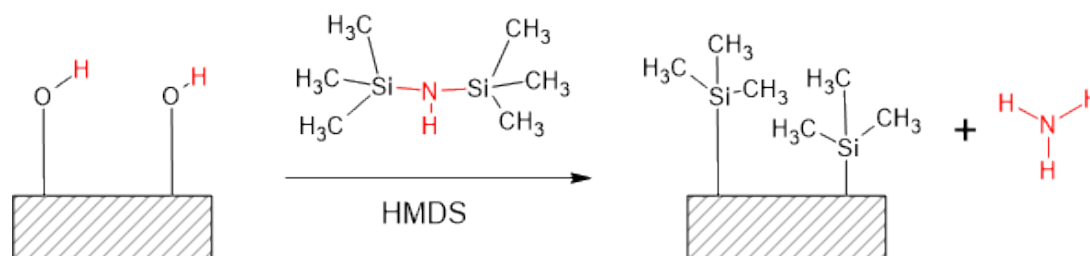
Fig. 1. The scheme of silica surface hydrophobization with HMDS

It is known that hexamethyldisilazane hydrolyses in humid air to trimethylsilanol (TMS) and ammonia (Seguin et al., 2008). Thus, the modified surface should be water-free because in the presence of adsorbed water molecule the reaction can lead to trimethylsilanol which will stay physically bonded to the surface for a short time. According to the nonpolar nature of the trimethylsilyl (−Si(CH$_3$)$_3$) group, the surface free energy after modification and thus its wettability will depend on the residual unreacted silanol groups, modification rate (yield) and distribution of the trimethylsilyl groups along the surface (Silverio et al., 2019). HMDS is also used in order to increase adhesion of the photoresist on the silicon wafer surface in the photolithography and the process known as the vapour prime takes place in a special prime oven to which the HMDS is supplied with nitrogen from a bubbler. Therefore, it is interesting to note how the silica surface will behave in a similar way.

The aim of this paper was to fabricate transparent and hydrophobic polysiloxane coatings on the glass supports. The dip-coating method was used for coating deposition from the composition synthesized by the tetraethoxysilane acid-assisted hydrolysis via the sol-gel method. The sol stability was investigated using the Turbiscan^{Lab} apparatus and its particle size was determined using the dynamic light scattering method. The coatings were hydrophobized by hexamethyldisilazane with two methods: the HMDS vapour deposition in a desiccator and the technique based on the silicon wafer treating. The obtained surfaces were characterized by wettability and transmission measurements as well as photoacoustic spectroscopy for hydrophobization efficiency determination.

2. Materials and methods

2.1. Materials

The following reagents and materials were used during the experiment:
- redistilled water

- *Milli-Q™* ultrapure water (18.2 MΩ·cm at 298K)
- acetone (99%, *POCH S.A.*, Poland)
- methanol, MeOH (99%, *POCH S.A.*, Poland)
- chloroform (98%, *POCH S.A.*, Poland)
- tetraethoxysilane, TEOS (98%, *Aldrich*)
- hydrochloric acid, HCl (35-38%, *POCH S.A.*, Poland)
- ethanol, EtOH (96%, *POCH S.A.*, Poland)
- hexamethyldisilazane, HMDS (98%, *Aldrich*)
- nitrogen (compressed, ALPHAGAZ™1, *AirLiquide*, Poland)
- glass microscope slides (*Comex*, Poland)

2.2. Fabrication of the surfaces

2.2.1. Purification of the supports

Microscope glass slides with the dimensions of 76x26x1 mm made by Comex (Poland) were used as the supports. Each slide was purified before the coating applied as follows: it was washed in an ultrasonic bath (cleaner) in acetone for 15 minutes, then in methanol for 15 minutes. Next, it was rinsed with the chloroform. After this procedure, the supports were dried at ambient temperature and the coatings were applied.

2.2.2. Synthesis of the sol

The composition used for the coating was synthesized by the sol-gel method. The sol was formed by hydrochloric acid-assisted hydrolysis of a precursor, which was the tetraethoxysilane (TEOS). The synthesis was performed as follows: 20.664 cm^3 of TEOS was poured into the vessel, then 1.812 cm^3 of redistilled water and 4.524 cm^3 of 1M HCl were added. The composition was stirred using a magnetic stirrer at 300 rpm at 50 °C for 2 hours. These volumes correspond to the molar ratio of $1.0:4.6\cdot10^{-2}:3.45$ for the TEOS : HCl : H_2O mixture (Chodkowski et al., 2019). Then 81.0 cm^3 of ethanol was instilled which corresponds to the volume dilution of 1:3, and the composition was still stirred at 600 rpm for 30 minutes at 50 °C. Next, the composition was divided into three equal volume parts and it was ready for coating.

2.2.3. Dip-coating

The glass supports were covered by the dip-coating using KSV NIMA KN4001 Dip Coater made by Biolin Scientific (Sweden). This is a compact, single vessel apparatus with the computer controlled dipping mechanism allowing for the sample withdrawal in the speed range of 0.1 mm/min to 1000 mm/min. The glass supports were successively immersed in a 36 cm^3 vessel containing the obtained sol to a depth of 56 mm and then they were withdrawn with a constant set speed. The withdrawal speeds of the samples are shown in Table 1 below. During the coating process the sol was still being stirred at 300 rpm and its temperature was kept at 50°C.

Table 1. The withdrawal speeds of the samples

Withdrawal speed [mm/min]	Sample #
20	1, 2, 3, 4, 9
50	5, 6, 7, 8, 10

After the covering the obtained surfaces were dried at room temperature for 24 h in a closed and ventilated chamber in order to prevent deposition of impurities and dusts.

2.2.4. Hydrophobization of the surfaces

The coatings were modified with hexamethyldisilazane in order to impart hydrophobicity. The samples 1, 2, 5, and 6 were kept in a desiccator at ambient temperature and pressure under HMDS vapour for 24 hours. After that, the unbound hexamethyldisilazane and the by-product (ammonia) were removed by heating the plates at 100°C for 1 hours. Samples 3, 4, 7, and 8 were hydrophobized at an elevated

temperature using a bubbler as follows: the plates were put into a closed glass container stored at 100°C in a laboratory oven; then the flow of the nitrogen used as a carrier gas was established at about 4 dm^3/min for 5 minutes in order to purify the chamber (glass container). Next, HMDS was added into the bubbler and the surface was exposed to the flowing gas mixture for 5 minutes. Finally, the bubbler was disconnected, and the pure nitrogen purged the chamber for another 5 minutes. The installation is shown schematically in Fig. 2 below.
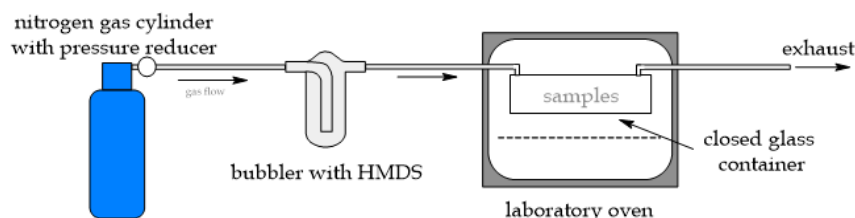
Fig. 2. Scheme of the apparatus for the surface hydrophobization at an elevated temperature

Samples 1, 3, 5, and 7 were additionally placed in a vacuum oven at the 100 mbar pressure at 60 °C for 2 hours in order to remove adsorbed or residual water before the hydrophobization. In this way there were obtained ten surfaces: eight hydrophobized with HMDS and two nonmodified as a control sample. A summary of the hydrophobization methods for each sample is presented in Table 2 below.

Table 2. Summary of the surface modification methods

Sample #	Drying	HMDS hydrophobization	Post-heating
1	vacuum	desiccator	yes
2	ambient	desiccator	yes
3	vacuum	bubbler + oven	no
4	ambient	bubbler + oven	no
5	vacuum	desiccator	yes
6	ambient	desiccator	yes
7	vacuum	bubbler + oven	no
8	ambient	bubbler + oven	no
9		non-modified	
10		non-modified	

2.3. Measurements with the Turbiscan^{LAB}

The Turbiscan^{LAB} apparatus made by Formulaction (France) equipped with the Turbiscan^{LAB} Cooler cooling/heating module was used in order to investigate the sol-gel composition stability. It allows fast and sensitive identification of destabilization processes and their mechanisms in the sample. The measuring principle is based on the light-scattering detection. The sample is placed in a 20 ml glass vessel and it is put into a thermostated measuring chamber. Then at given intervals for a specified period along the vertical axis from the bottom to the top of the vessel a diode emitting light with a wavelength of 850 nm is moving. Every 20 µm transmission (T) through the sample and backscattering (BS) at an angle of 135 degrees are registered. To analyse transparent or turbid dispersions transmission is used while backscattering is helpful to examine opaque ones (Polowczyk et al., 2015). Based on the transmittance or backscattering profiles it is possible to calculate the Turbiscan Stability Index (TSI). This dimensionless parameter estimates the stability of the sample and allows to compare the samples with each other. The TSI values are within the range from 0 to 100. The higher the TSI value, the more unstable the sample is (Wiśniewska et al., 2013). The manufacturer's instruction specifies the TSI value in the range 1-3 as "Visual Pass" which means beginning of the destabilization, but it remains invisible for the eye. Over this range (above 3) the destabilization can become visible. The stability measurements were made as follows: the obtained sol was put into the Turbiscan vessel immediately after the end of the synthesis and the measurements were made at 50 °C, in parallel with the dip-coating. Transmission profiles were collected for 3 h every minute and then for 21 h every 30 minutes. After that, the sample

was stored in a dark place at 20 °C and after 14 days transmission profiles were registered for 15 h every 15 minutes. The TSI was calculated based on the transmission profiles by the TurbiSoft 2.3 software as follows (Saidi et al., 2020):

$$TSI = \frac{[\sum_h scan_i(h) - scan_{i-1}(h)]}{H} \tag{1}$$

where i is the scan number, h is the transmittance at every measured position, H is the total sample height. The global TSI involves all single measurements averaged during the experiment time.

2.4. Particle size analysis

The particle size determination was made using the Zetasizer Nano ZS90 (Malvern Instruments Ltd., Malvern, UK). It is based on the Dynamic Light Scattering (DLS) measurements known also as photon correlation spectroscopy (PCS) or quasi-elastic light scattering (QELS) at a 90-degree scattering angle. This technique measures the diffusion of particles moving with the Brownian motion and converts this to particle size and its distribution using the Stokes-Einstein relationship. The measurements were made at 50 °C using the 40 µl disposable micro cuvette. In the software ethanol was set as the dispersant with its refraction index value equal to 1.362; the viscosity was taken from the software database. The sample was taken immediately after the end of the synthesis and the measurements were made in parallel with the dip-coating.

2.5. Wettability measurements

The differences in surface properties can be determined by the contact angle measurements (Sadowski et al., 2018). They were made using the DigiDrop Contact Angle Meter (GBX, France). The contact angles were calculated by the WinDrop++ software based on the droplet shape using the fixed base mode. The measurements were performed at room temperature applying the sessile droplet method as follows: the Milli-Q ultrapure water droplet of 6 µl volume was settled on the examined surface using a microsyringe and the advancing contact angle was measured; then 3 µl of liquid was sucked into the microsyringe and the receding contact angle was measured. In this way eight water droplets were measured and averaged along each surface. For more accurate characterization of the surface wettability, the equilibrium contact angles on each sample were calculated using the Tadmor approach (Tadmor, 2004) based on the pair: the advancing and corresponding receding contact angles.

2.6. Photoacoustic spectroscopy (PAS)

The Excalibur FTS 3000MX FT-IR spectrometer made by Bio-Rad (USA) was used in order to record the Fourier transformed photoacoustic infrared (FT-IR/PAS) spectra of the samples. They were recorded at room temperature, over the 4000-400 cm^{-1} range, with the resolution 4 cm^{-1}, mirror velocity 2,5 kHz and maximum source aperture, using the MTEC Model 300 photoacoustic cell. Each sample was placed in a stainless-steel cup (diameter 10 mm) and dry helium was used to purge the photoacoustic cell before the data acquisition. Then the interferograms of 1024 scans were averaged for the spectrum in order to provide a good signal-to-noise (S/N) ratio. Despite the fact that the data were recorded using the same settings and set of parameters, and the sample sizes were identical, the resulted spectra were normalized using the band attributed to the symmetric stretching vibrations of (Si–O-Si) bonds at about 793 cm^{-1} (Rubio et al., 1998) for an internal standard. The baseline subtraction was made by OriginLab software using the Asymmetric Least Squares Smoothing Baseline (ALS) method.

2.7. Transmission properties measurements

The transmission measurements of the samples were made using Helios Gamma Spectrophotometer made by Thermo Electron Corporation (USA). It is a UV-Vis spectrophotometer equipped with the quartz coated single-beam optical system. It is characterised by the 2 nm spectral bandwidth; tungsten lamp and deuterium lamp are used as a light source. The spectra were taken at room temperature, with 0.5 nm step in the range of wavelength from 190 nm to 1100 nm which corresponds to the radiation from the ultraviolet (UVC), through the visible light, to near infrared (NIR or IR-A). Before the measurements of the samples the baseline was measured and then it was subtracted from the resulted

spectra automatically in order to remove the noise present in the background which is not related with the samples. The data was collected by a PC with the installed VISION software.

3.   Results and discussion

3.1. Measurements with the TurbiscanLAB

Fig. 3 below shows the Turbiscan transmission data of the sol-gel composition for 24 hours directly after the end of the synthesis.
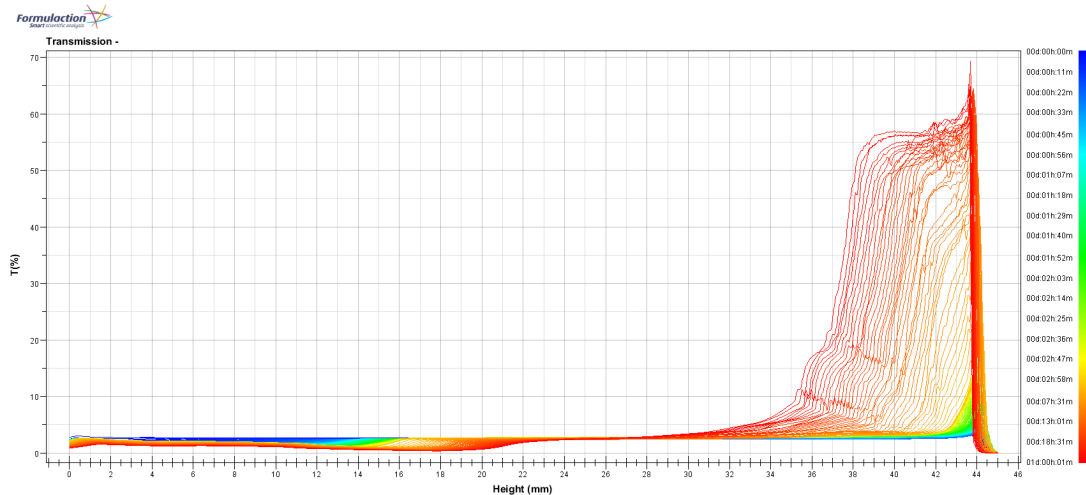
Fig. 3. Transmission of the sol-gel composition after the fabrication

In the upper part of the sample there can be observed an increase in transmission which intensifies after about 3 hours from the moment of the end of the composition synthesis. It is a formation of a clear layer of the solvent in the top of the flask with a density lower than that of the gel caused by the inability to evaporate ethanol (closed vessel) during th e gelation. The interface established at the height of about 28 mm and then it was moving down to the middle of the flask. The transmission changes in the lower sample layer, characteristic of the particle migration or diameter changes, correspond to the gel thickening. The global TSI after 24 hours is equal to 11.40 which indicates that the composition is unstable. However, the same parameter for the first 20 minutes is equal to only 0.1. This indicates that no significant changes or destabilization occur in the solution during the application of the coatings. Thus, not mixing the composition during the dip-coating can be considered. Observation of the transmission profiles allows the conclusion that the polymerization process in the solution was completed. The instability of the system results from phase separation, which is the effect of the initiation of the gelation, not the growth of the polymer chain. This indicates that the reaction time is suitable and sufficient for a given temperature.

The gelation of the composition was completed 14 days after its synthesis. In Fig. 4, the step change of the transmission can be observed at half the height of the flask. This is the interface between the gel and the solvent – the ethanol phase. The transmission of the gel layer is practically equal to zero which indicates a non-transparent medium of high density and viscosity and its values of the clarified ethanol layer are maintained at a high level which confirms the complete separation of the two phases.
Both phases are stable because the transmission does not change for 15 hours and the graphs practically overlap. Gelation and the completion of the solvent clarification are confirmed by the appropriate indicators - the global TSI for the gel layer after 15 hours is equal to 0.0 and for the ethanol layer is equal to 0.7.

3.2. Particle size analysis

The obtained particle size distribution is shown in Fig. 5 below. Only one peak can be found; it is symmetrical and relatively narrow. The mean particle size is equal to 3.1 nm with the standard deviation

equal to 0.5 nm. On the other hand, the polydispersity index (PdI) is equal to 0.9 and the z-Average diameter value (Z_D) is equal to 8.4×10^4 nm.
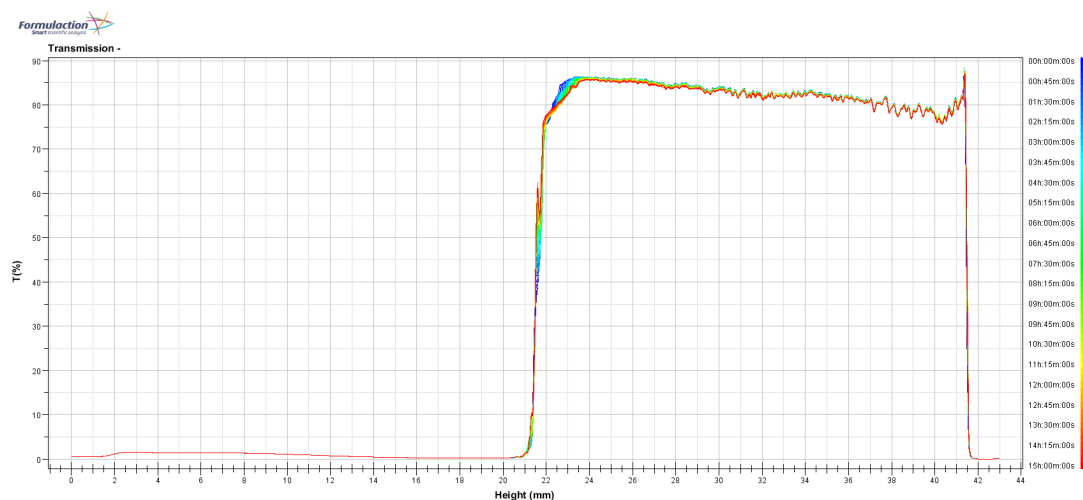
Fig. 4. Transmission of the sol-gel composition after 14 days
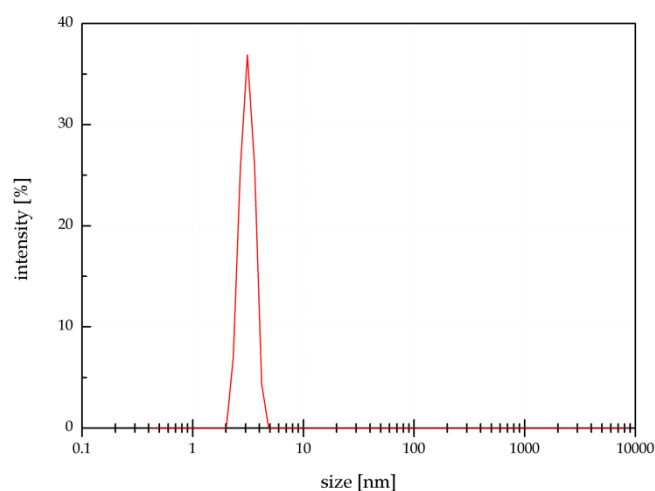
Fig. 5. Particle size distribution by intensity

It should be kept in mind that the parameter indicated as a particle size determined by this technique is in fact the hydrodynamic diameter (or radius). This approach assumes the particle to be as hard sphere. In case of a polymer, it is not the same as the radius of gyration. Converting the hydrodynamic size to the radius of gyration there must be considered several parameters such as the polymer chain structure (degree of branching) and its conformations (random coil, chain stiffness etc.). It was proved that the diffusion coefficient which is taken for the hydrodynamic size calculations based on the Stokes-Einstein relationship depends on the liquid-particle interactions. Thus, the strong binding energies in the system can lead to some overestimations. For this reason, the results reported in the literature can be sometimes considered as controversial (Li, 2009). The Stokes-Einstein relationship validity is well acknowledged for simple fluids, but some authors claim that this is not the precise law and they propose some corrections (Zhao and Zhao, 2020). On the other hand, the z-Average diameter is very sensitive to the presence of aggregates. The polydispersity index value close to 1 indicates that the sample has a very broad size distribution. According to the obtained results, the DLS technique does not appear to be a suitable method for analyzing this type of systems.

3.3. Wettability measurements

The advancing and receding contact angles on the samples and the contact angle hysteresis directly after the coating fabrication as well as after 14 days are presented in Figs. 6 and 7, respectively.
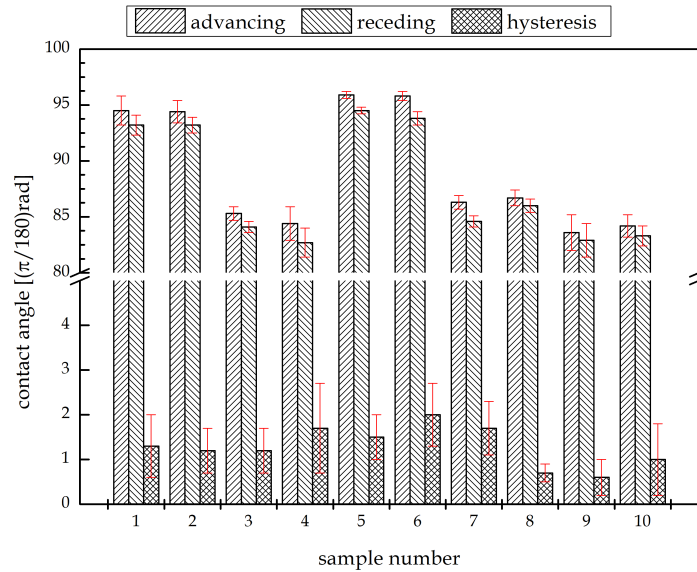
Fig. 6. Wettability of the samples directly after the coatings fabrication process
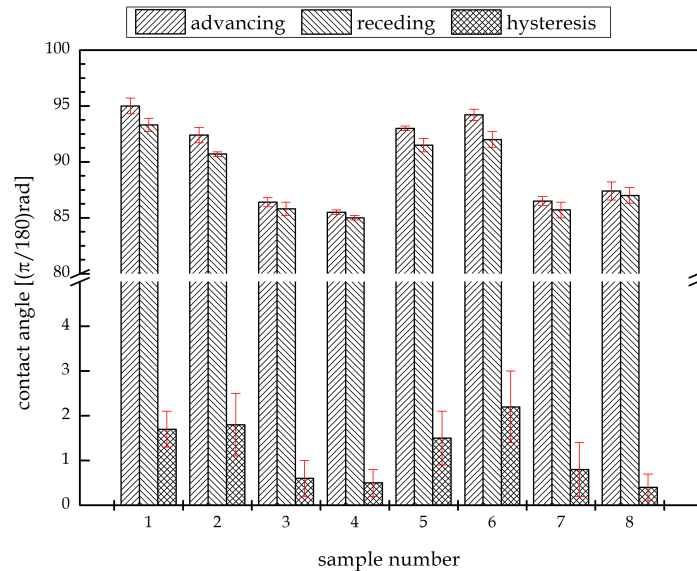
Fig. 7. Wettability of the samples a week after the fabrication

The parameters and structure of the obtained coatings will depend on the conditions of the reaction of the precursor hydrolysis. The acid-assisted TEOS hydrolysis leads to a linear polymer instead of silica nanoparticles which are formed during the base-assisted reaction (Cai et al., 2014). In the case of linear polymer compositions, dense and smooth coating layers are obtained. This is confirmed by the low contact angle hysteresis on all surfaces (in the range 0.4-2.2 degrees) which indicates both chemical and physical homogeneity as well as smoothness of the coatings.

The advancing and receding contact angles provide a description of the surface energy and roughness degree of a solid. Thus this is necessary for meaningful estimation of the mean wettability of the system in a different way (Montes Ruiz-Cabello et al., 2014). It should be kept in mind that it is impossible to measure the Young contact angle (Young, 1805) due to its correspondence to the ideal and physically unachievable model of the liquid droplet on the solid surface (Della Volpe et al., 2001; Bormashenko, 2013). There are various theories for predicting the equilibrium contact angle (Bormashenko, 2020; Drelich et al., 2020) but the Tadmor's approach was used. The obtained equilibrium contact angles are shown in Fig. 8.

According to the Fig. 8 above, the best hydrophobization effect can be observed using samples 1, 2, 5 and 6. They were modified by their storage under HMDS vapors in the desiccator. In this case, the
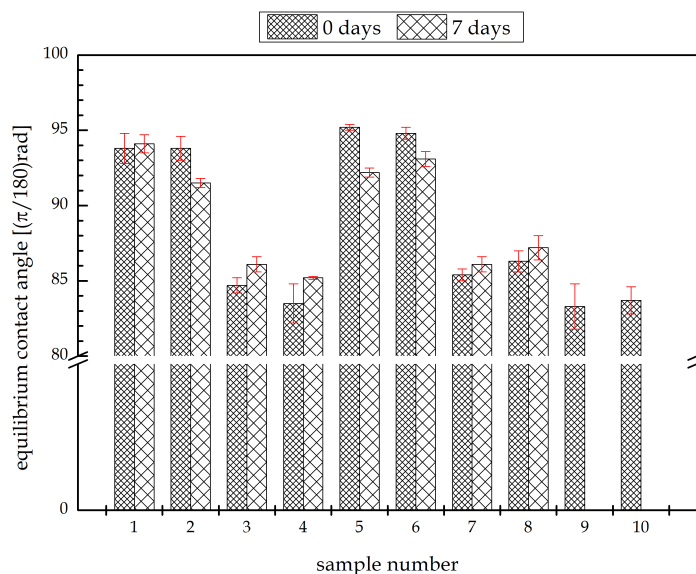
Fig. 8. The equilibrium contact angles of water on the samples

effect of a slight decrease in hydrophobicity after 14 days appears due to volatilizing the modificator which was only physically bound to the surface according to the two-step reaction mechanism (Gun'ko et al., 2000). Because of the contact angle values greater than 90 degrees for surfaces 1, 2, 5 and 6 they can be considered as hydrophobic ones. The surface modification with HMDS using a bubbler at an elevated temperature resulted in worse hydrophobization results. The contact angles are about 10 degrees lower than with the samples modified with hexamethyldisilazane vapours in the desiccator. The increase in hydrophobicity after 14 days may results from the fact that during a short modification time (5 minutes) some HMDS molecules remained chemically unbound with the surface, just stayed adsorbed there. The lack of post-heating of the sample did not cause volatilization of the adsorbed modifier which then allowed for its chemical binding to the surface. After 14 days of the coatings fabrication, the highest contact angle of 94.1 degrees was characteristic of the sample number 1 which means the best hydrophobization effect. This is also confirmed by the PAS spectra, where the highest intensity in the range of methyl groups can be observed for this sample.

Although the hydrophobic effect on surface number 1 did not decrease, for the surface 5 modified in the same way the lower contact angle values after 14 days can be found whereas on all surfaces hydrophobized with the bubbler at an elevated temperature the contact angle increased slightly. Thus, in both cases, it can not be clearly stated whether storing the samples under vacuum conditions before the modification affects the efficiency of surface hydrophobization.

It is well known that the withdrawal speed during dip-coating determines the layer thickness and its mechanical properties. For the silica-based coatings fabrication there is a critical withdrawal speed range from about 20 mm/min to 50 mm/min. Under these conditions homogeneous, transparent, and crack-free films with a minimum thickness can be obtained (Figus et al., 2015). As it can be seen in Fig. 7, there is a negligible difference in the contact angle values among samples 9 and 10, 3 and 7, 4 and 8. These pairs of surfaces differ only in the withdrawal speed. Thus, it can be concluded that the withdrawal speed within the critical range has no effect on the wettability of the obtained coatings.

3.4. Photoacoustic spectroscopy

The full ranges of the PAS spectra have not been presented because with such a selected scale the graphs practically coincide. Moreover, the range below 1300 cm^{-1} does not seem interesting due to the presence of bands described as a superimposition of various SiO_2 peaks, among others, the bands corresponding to the Si–O–Si bond asymmetric stretching in the region from 1300 to 1000 cm^{-1} (Capeletti and Zimnoch, 2016). The most interesting from the point of view of surface modification is the range of 3700 to 2700 cm^{-1}. The area of 3000–2800 cm^{-1} covers stretching of C–H bonds in alkanes whereas 3700–3100 cm^{-1} corresponds to stretching of O–H bonds in water. In fact, there are two strong peaks at 2850 cm^{-1} and

2930 cm^{-1} originating from the methyl groups on the surface. Unfortunately, there are also broad bands in the 3600-3100 cm^{-1} range which corresponds to the hydrogen-bonded clusters of water. They come from the water molecules adsorbed on the surface and cover the sharp peak at 3690 cm^{-1} assigned to the stretching of O–H bonds in the isolated surface hydroxyl groups and overlap the range 3400–3200 cm^{-1} which corresponds to the hydrogen-bonded –OH surface groups in the Si–O–H structure (Launer and Arkles, 2013). The surface hydrophobization consisted in replacing the surface hydrophilic hydroxyl groups (–OH) with the hydrophobic methyl groups (–CH$_3$). Thus, the lower the content of –OH groups in favour of –CH$_3$ groups, the higher the modification efficiency (hydrophobization) should be. The highest intensity of methyl groups for sample number 1 can be observed; this confirms the hydrophobicity from the wettability measurements (the highest contact angles and effect stability in Fig. 8). The high intensities in the case of samples number 4, 5 and 6 are also observed. For surfaces 5 and 6 this corresponds to the wettability results whereas the contact angle was the smallest on surface number 4. It should be noted here that the final hydrophobic effect is influenced by the ratio of methyl groups to the irreplaceable hydroxyl groups on the surface.
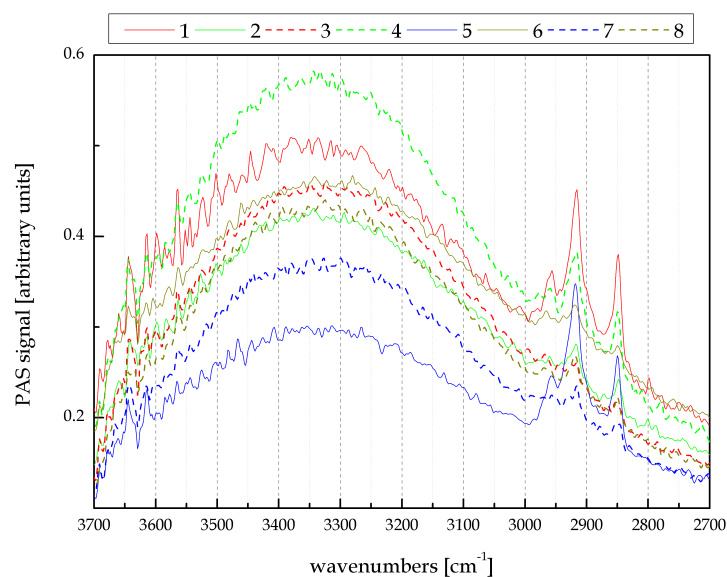
Fig. 9. Photoacoustic spectra of the samples in the range from 2800 to 3500 cm^{-1}

Therefore, the highest peak intensity in the –CH$_3$ region does not necessarily mean the most hydrophobic surface and the best modification effect. Due to the presence of a broad band in the range coming from various states of –OH groups, it is not possible to identify individual peaks originating from the unassociated surface hydroxyl groups and thus to compare the surface modification degree. The above results also show that even after a short period from the removal of samples from an inert atmosphere or a desiccator, the water present in the air is adsorbed on their surface. Therefore, before performing the PAS analysis, the samples should be stored under vacuum or argon and transferred directly to the inert atmosphere in the chamber of the measuring apparatus.

3.5. Transmission properties measurements

As it can be observed in Fig. 10, the transmission for the samples in the visible light range remains at a practically constant and high level. It is characterized by a wide maximum in the region of 350–1100 nm. The minimum in the 190–350 nm range can be related with the absorption in the glass support (Olenych et al., 2017). This takes place because of its composition – most glass contains silicon dioxide and sodium dioxide. Combination of these components results in the material with a band gap around 4 eV which is able to absorb wavelengths shorter than about 310 nm (Kumar, 2012). This range corresponds to the UV light excluding UVA – the least dangerous type of UV light.

In Fig. 11 an enlarged graph in the visible light range is presented. There are some differences in the transmission within a few percent between the samples. It can be observed that the covered samples are characterized by higher transmission. Moreover, the modified (hydrophobized) coatings have better
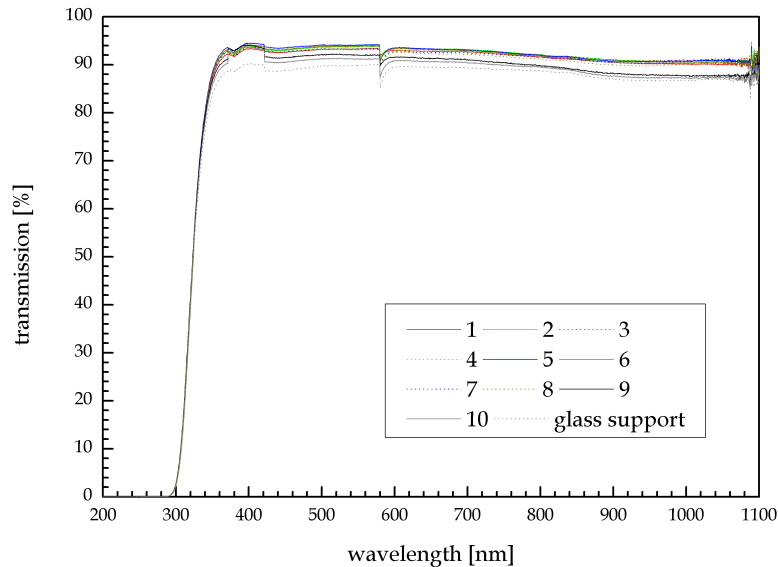
Fig. 10. Transmission spectra of the samples

transmission properties than the nonmodified ones. It means that introducing methyl groups onto the surface during the modification process improves not only the hydrophobicity but also the transmission properties of the coating. The transmission differences within the modified surfaces are small – of about 1 percent and may result from measurement conditions, therefore they will not be discussed further. Covering the glass support with the synthesized coating results in an increase in transmission, therefore it can be considered as an anti-reflective (AR) coating (Tao and Zhang, 2020). These types of coatings are called transmission or light boosters because they can increase the light transmission through a lens or just glass – in the case of polysiloxane-based ones up to 98% (Yuan et al., 2020).
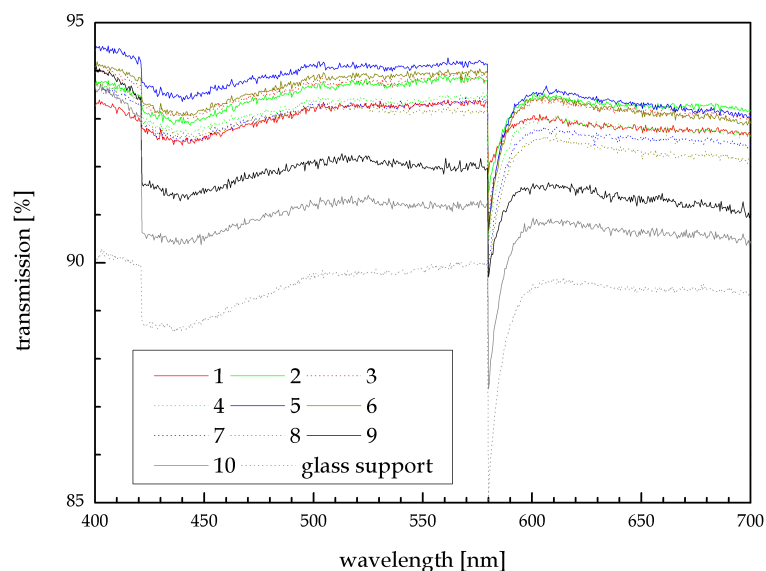
Fig. 11. Transmission spectra of the samples zoomed in the visible light range

The sharp peak at 580 nm appears to be due to silicon oxygen hole centers in the supports made during the glass production process (Carter and France, 1983); this effect is the strongest for the uncovered glass slide and is slightly counteracted by the applied coating.

4. Conclusions

Silica layers on the glass supports were fabricated using the fast and convenient sol-gel dip-coating method. The synthesized sol showed good stability applying the coatings and the TEOS hydrolysis was

complete. Its entire gelation took place after 14 days from the synthesis. The DLS measurements do not seem to be a suitable technique for particle size determination due to the presence of the linear form (chains) of the polymer in the sol. The surface modification at an elevated temperature with HMDS using a bubbler provides worse effects than deposition of its vapours in a desiccator. In the former case, surfaces with a water contact angle lower than 90 degrees were obtained while in the latter case the hydrophobic surfaces were produced. The effectiveness of this modification was partially confirmed by the PAS spectra. The best result was obtained in the case of hydrophobization of the sample in a desiccator with HMDS vapours preceded by their storage under the vacuum condition. The low contact angle hysteresis indicates obtaining smooth and uniform coatings. The fabricated samples are also characterized by better transmission properties than the glass supports, therefore the coatings can be considered anti-reflective.

References

BORMASHENKO, E., 2013. *Wetting of real solid surfaces: new glance on well-known problems*. Colloid Polym. Sci. 291, 339–342.

BORMASHENKO, E., 2020. *Variational framework for defining contact angles: a general thermodynamic approach*. J. Adhes. Sci. Technol. 34(2), 219–230.

CAI, S., ZHANG, Y., ZHANG, H., YAN, H., LU, H., JIANG, B., 2014. *Sol–Gel Preparation of Hydrophobic Silica Antireflective Coatings with Low Refractive Index by Base/Acid Two-Step Catalysis*. ACS Appl. Mater. Interfaces 6(14), 11470–11475.

CAPELETTI, L.B., ZIMNOCH, J.H., 2016. *Fourier transform infrared and Raman characterization of silica-based materials*, in *Applications of Molecular Spectroscopy to Current Research in the Chemical and Biological Sciences*. IntechOpen, London, UK, https://doi.org/10.5772/64477.

CARTER, S.F., FRANCE, P.W., 1983. *Drawing induced absorption loss in multicomponent glass fibres*. J. Non-Cryst. Solids 58(1), 47–55.

CHODKOWSKI, M., TERPIŁOWSKI, K., GONCHARUK, O., 2019. *Surface properties of the doped silica hydrophobic coatings deposited on plasma activated glass supports*. Physicochem. Probl. Miner. Process. 55(6), 1450–1459.

DELLA VOLPE, C., MANIGLIO, D., SIBONI, S., MORRA. M., 2001. *An Experimental Procedure to Obtain the Equilibrium Contact Angle from the Wilhelmy Method*. Oil & Gas Science and Technology – Revue de IFP Energies Nouvelles 56(1), 9–22.

DRELICH, J.W., BOINOVICH, L., CHIBOWSKI, E., DELLA VOLPE, C., HOŁYSZ, L., MARMUR, A., SIBONI, S., 2020. *Contact angles: history of over 200 years of open questions*. Surf. Innov. 8(1–2), 3–27.

FIDALGO, A., ILHARCO, L.M., 2004. *Chemical Tailoring of Porous Silica Xerogels: Local Structure by Vibrational Spectroscopy*. Chemistry – A European Journal 10, 392–398.

FIGUS, C., PATRINI, M., FLORIS, F., FORNASARI, L., PELLACANI, P., MARCHESINI, G., VALSESIA, A., ARTIZZU, F., MARONGIU, D., SABA, M., MARABELLI, F., MURA, A., BONGIOVANNI, G., QUOCHI, F., 2015. *Synergic combination of the sol–gel method with dip coating for plasmonic devices*. Beilstein J. Nanotechnol. 6, 500–507.

GUN'KO, V.M., VEDAMUTHU, M.S., HENDERSON, G.L., BLITZ, J.P., 2000. *Mechanism and Kinetics of Hexamethyldisilazane Reaction with a Fumed Silica Surface*. J. Colloid Interface Sci. 228(1), 157–170.

IBRAHIM, S., SULTAN, M., 2020. *Superhydrophobic Coating Polymer/Silica Nanocomposites: Part I Synthesis and Characterization as Eco-Friendly Coating*. Silicon 12, 805–811.

KUMAR, V., 2012. *Optical and invitro bioactive properties of sodium silicate glasses*. Indian J. Pure Appl. Phys. 50, 335–338.

LAUNER, P., ARKLES, B., 2013. Infrared *Analysis of Organosilicon Compounds*, in: *Silicon Compounds: Silanes & Silicones*. Gelest Inc., Morrisville, USA.

LEGGE, C.J., COLLEY, H.E., LAWSON, M.A., RAWLINGS, A.E., 2019. *Targeted magnetic nanoparticle hyperthermia for the treatment of oral cancer*. J. Oral Pathol. Med. 48, 803–809.

LI, Y., ZHANG, L., LI, C., 2020. *Highly transparent and scratch resistant polysiloxane coatings containing silica nanoparticles*. J. Colloid Interface Sci. 559, 273–281.

LI, Z., 2009. *Critical particle size where the Stokes-Einstein relation breaks down*. Phys. Rev. E 80, 061204.

MONTES RUIZ-CABELLO, F.J., RODRÍGUEZ-VALVERDE, M.A., CABRERIZO-VÍLCHEZ, M.A., 2014. *Equilibrium contact angle or the most-stable contact angle?*. Adv. Colloid Interface Sci. 206, 320–327.

OLENYCH, I., AKSIMENTYEVA, O., MONASTYRSKII, L., HORBENKO, Y., PARTYKA, M., 2017. *Electrical and Photoelectrical Properties of Reduced Graphene Oxide – Porous Silicon Nanostructures*. Nanoscale Res. Lett. 12, 272.

POLOWCZYK, I., BASTRZYK, A., KOŹLECKI, T., SADOWSKI, Z., 2015. *Stability of Three-Phase Water-Particle-Oil Systems*. Chem. Eng. Technol. 38(4), 715–720.

PROTSAK, I., PAKHLOV, E., TERTYKH, V., LE, Z., DONG, W., 2018. *A New Route for Preparation of Hydrophobic Silica Nanoparticles Using a Mixture of Poly(dimethylsiloxane) and Diethyl Carbonate*. Polymers 10(2), 116.

RUBIO, F., RUBIO, J., OTEO, J.L., 1998. *A FT-IR Study of the Hydrolysis of Tetraethylorthosilicate (TEOS)*. Spectrosc. Lett. 31(1), 199–219.

SADOWSKI, Z., BARANSKA, J., PAWLOWSKA, A., 2018. *Surface properties of neutral components in copper column bioleaching of black shale samples*. Physicochem. Probl. Miner. Process. 54(4), 1146–1151.

SAIDI, M.Z., PASC, A., EL MOUJAHID, C., CANILHO, N., BADAWI, M., DELGADO-SANCHEZ, C., CELZARD, A., FIERRO, V., PEIGNIER, R., KOUITAT-NJIWA, R., AKRAM, H., CHAFIK, T., 2020. *Improved tribological properties, thermal and colloidal stability of poly-a-olefins based lubricants with hydrophobic MoS_2 submicron additives*. J. Colloid Interface Sci. 562, 91–101.

SAN VICENTE, G., BAYÓN, R., GERMÁN, N., MORALES, A., 2011. *Surface modification of porous antireflective coatings for solar glass covers*. J. Sol. Energy 85(4), 676–680.

SEGUIN, K., DALLAS, A., WEINECK, G., 2008. *Rationalizing the mechanism of HMDS degradation in air and effective control of the reaction byproducts*, https://doi.org/10.1117/12.772998.

SILVERIO, V., A.G. CANANE, P., CARDOSO, S., 2019. *Surface wettability and stability of chemically modified silicon, glass and polymeric surfaces via room temperature chemical vapor deposition*. Colloids Surf. A Physicochem. Eng. Asp. 570, 210–217.

TADMOR, R., 2004. *Line Energy and the Relation between Advancing, Receding, and Young Contact Angles*. Langmuir 20(18), 7659–7664.

Tao, Ch., Zhang, L., 2020. *Fabrication of multifunctional closed-surface SiO_2–TiO_2 antireflective thin films*. Colloids Surf. A Physicochem. Eng. Asp. 585, 124045.

WIŚNIEWSKA, M., TERPIŁOWSKI, K., CHIBOWSKI, S., URBAN, T., ZARKO, V.I., GUN'KO, V. M., 2013. *Stability of Colloidal Silica Modified by Macromolecular Polyacrylic Acid (PAA) – Application of Turbidymetry Method*. J. Macromol. Sci. A 50(6), 639–643.

YANG, J., LI, J., XU P., CHEN, B., 2020. *Robust and transparent superoleophobic coatings from one-step spraying of SiO_2@fluoroPOS*. J. Sol-Gel Sci. Technol. 93, 79–90.

YOUNG, T., 1805. *An essay on the cohesion of fluids*. Philos. Trans. R. Soc. Lond. 95, 65–87.

YUAN, J., YAN, S., ZHANG, X., 2020. *Superhydrophilic antifogging broadband antireflective coatings with worm-like nanostructures fabricated by one dip-coating method and calcination*. Appl. Surf. Sci. 506, 144795.

YUE, D., FENG, Q., HUANG, X., ZHANG, X., CHEN, H., 2019. *In Situ Fabrication of a Superhydrophobic ORMOSIL Coating on Wood by an Ammonia–HMDS Vapor Treatment*. Coatings 9(9), 2079–6412.